# Statistical Acquisition of DVB-S2X Signal for Positioning in LEO-NTN

1st Harshal More*, 2th Idir Edjekouane †, 3 nd Ernestina Cianca*, 4 rd Mauro De Sanctis*,
5th Jorge Querol†, 6th Ottavio Picchi‡, 7th Francesco Menzione‡
*Dept. Electronics Engineering, Torvergata University, Rome, Italy
† SnT, University of Luxembourg, Luxembourg
‡JRC, European Commission, Ispra, Italy
Email: Harshal More, harshalshyamsundar.more@alumni.uniroma2.eu

2025 International Conference on Localization and GNSS (ICL-GNSS) | 979-8-3315-1113-5/25/$31.00 ©2025 IEEE | DOI: 10.1109/ICL-GNSS65520.2025.11046183

***Abstract*—Low Earth Orbit (LEO) mega-constellations are revolutionizing global communication by delivering high-speed internet and supporting a wide range of services. Beyond communication, recent studies have shown that LEO satellites can also provide Positioning, Navigation, and Timing (PNT) services. Leveraging existing LEO Non-terrestrial-network (NTN) for dual-purpose applications has garnered significant attention as a future-oriented approach. This paper investigates the feasibility of re-purposing a well-established satellite communication protocol, Digital Video Broadcasting Second Generation Satellite Extensions (DVB-S2X), for positioning applications within LEO-NTN. This paper analyses the statistical acquisition performance similar to the Global Navigation Satellite System (GNSS) to evaluate the potential of DVB-S2X for positioning estimation. This analysis can provide a baseline for trade-offs for communication protocol selection when developing a sustainable integrated navigation and communication (Nav-Comm) system within LEO-NTN.**

***Index Terms*—Positioning, LEO-NTN, DVB-S2X superframe, Nav-Comm integration, Statistical Acquisition.**

## I. Introduction

Low Earth Orbit (LEO) mega-constellations are revolutionizing global communication by delivering high-speed internet and supporting a wide range of services. Beyond communication, recent studies have shown that LEO satellites can also provide Positioning, Navigation, and Timing (PNT) services, complementary to legacy Global Navigation Satellite Systems (GNSS). LEO-PNT can be implemented through various approaches, each with its advantages and limitations [1]. This work focuses on the Fused LEO-PNT approach where the existing satellite communication protocols can be exploited and repurposed for positioning service [2]–[4]. This integrated approach is sustainable as existing LEO Non-terrestrial-network (NTN) infrastructure can be used for dual purposes.

The MARINA project by ESA recently conducted a comparative analysis of the communication performance of $5^{th}$ Generation New Radio (5G-NR) and Digital Video Broadcasting - Second Generation Satellite Extensions (DVB-S2X) for their potential adaptation to LEO-NTN systems [5], [6]. Additionally, in [7] author emphasizes that most commercial LEO satellite communication systems achieve significant performance enhancements by using DVB-S2/S2X, developed by ETSI [8], [9]. However, 5G-NR has already demonstrated positioning capabilities through Signal of Opportunity (SoO) i.e, the use of Synchronization Signal Block (SSB) for acquisition and tracking [10] and dedicated Positioning Reference Signals (PRS) i.e., use of SSB for acquisition and PRS for tracking [11]. In contrast, the use of DVB-S2X for positioning remains largely unexplored, despite its well-established success, reliability, and adaptability in satellite communication [4].

This paper addresses the gap by exploring the feasibility of using DVB-S2X for positioning in LEO-NTN systems. It conducts a statistical signal acquisition analysis similar to GNSS, focusing on delay and Doppler estimation. The synchronization sequence (SS) at the start of the DVB-S2X superframe (SF), analogous to the pseudo-random noise (PRN) code in GPS C/A L1, is utilized for this purpose. The study evaluates and compares the acquisition performance of DVB-S2X and GPS C/A L1 codes using key metrics such as Auto-Correlation Functions (ACF), Receiver Operating Characteristics (ROC), and Mean Acquisition Time (MAT). It examines the effects of factors including operating signal-to-noise ratio (SNR), SS length, coherent integration time, SS periodicity, signal bandwidth (BW), acquisition losses due to misalignment of delay, and Doppler bins. ROC performance is validated through the Monte Carlo simulation. This preliminary analysis can provide a baseline for trade-offs for communication protocol selection when developing a sustainable integrated navigation and communication (Nav-Comm) system within LEO-NTN.

The paper is organized as follows: Section II briefly overviews the DVB-S2X superframe (SF) structure. Section III presents the downlink system model, a general statistical signal acquisition framework, which applies to DVB-S2X and GPS L1 C/A signals. It includes hypothesis testing, formulation of probabilities of false alarm and detection, acquisition losses for estimation of key performance metrics such as ROC and MAT. Section IV shows performance analysis and finally conclusion is drawn in Section V.

## II. Overview of DVB-S2X Frame Structure

DVB-S2X is an advanced digital satellite transmission standard based on its predecessor, DVB-S2 [8], [9].

979-8-3315-1113-5/25/$31.00 © 2025 IEEE

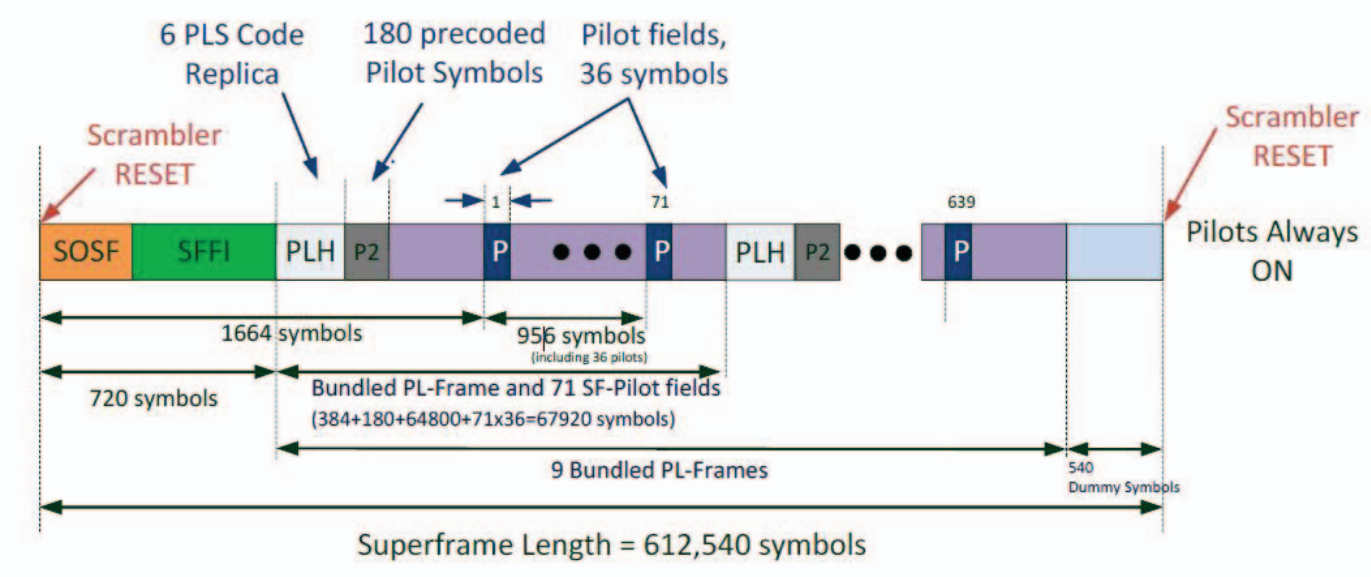


Fig. 1: Superframe (SF) of constant length independent of the choice of a SF format, which specifies the resource allocation and content [12]

This standard has a flexible SF structure that makes it efficient for modern satellite communication systems. [12]. SF has a constant length ($L_{SF}$) of 612,540 symbols as shown in Fig. 1. At the beginning of the frame, there is the Start-Of-Superframe (SOSF) and Superframe-Format-Indicator (SFFI) composed of 720 symbols. The remaining portion is allocated to the payload. The allocation of these symbols may vary depending on the format of the SF structure. SF can have 8 different formats, ranging from indices 0 to 7 and 8 to 15. Detailed information on each of these formats is found in [12]. The use of each format is application-based. In general, specific resource allocation contains Physical layer headers (PLHEADERs), Physical layer frames (PLFRAMEs), Pilot fields (P), etc. A Set of 90 symbols is called a capacity unit (CU), which is the basic element of SF. This CU is helpful for PLFRAMEs to establish (re)synchronization/search. The receiver performance is enhanced using this structure. Robust synchronization is achieved using SOSF, SFFI, and P. This work focuses on using the SOSF and SFFI for statistical acquisition, which are generated as follows:

- **SOSF**: SOSF has a length of 270 symbols, which is derived from the binary sequence of 256 bits orthogonal Walsh-Hadamard (WH) matrix ($H_{SOSF}$) with 14 padding symbols [13] to maintain the required length. WH matrix is constructed by:

$$H_{2m} = \begin{pmatrix} H_m & H_m \\ H_m & -H_m \end{pmatrix} \tag{1}$$

$$H_{256} = H_{2m} \otimes H_{2m} \otimes H_{2m} \otimes H_{2m} .. (\times 128) \tag{2}$$

where $\otimes$ is Kronecker product [14].

The padding matrix is generated by deleting the first and last columns of $H_{16}$, such that:

$$H_{14} = H_{16}(:, 1:14) \tag{3}$$

$$H_{padding} = \begin{pmatrix} H_{14}; & H_{14}; & H_{14}; & .... & H_{14} \end{pmatrix} \tag{4}$$

adding Eq. 2 and Eq. 4 WH matrix is estimated:

$$H_{SOSF} = \begin{pmatrix} H_{256}; & H_{padding} \end{pmatrix} \tag{5}$$

The matrix $H_{SOSF}$ hosts SOSF information row by row. The selection of each row is the static choice for the transmitted signal. SOSF is mapped to the Binary Phase Shift Keying (BPSK) modulation constellation by multiplying the selected sequence by $(1+j)/\sqrt{2}$.

- **SFFI**: The SFFI field is of length 450 symbols. The first 4 bits represent $b_{SFFI}$ which gives information about the format [12]. So, matrix $c_{SFFI}$ is such a that;

$$c_{SFFI} = b_{SFFI} * G_{sx} \tag{6}$$

where;

$$G_{sx} = \begin{pmatrix} 0000000 & 11111111 \\ 0001111 & 00001111 \\ 0110011 & 00110011 \\ 1010101 & 01010101 \end{pmatrix} \tag{7}$$

Each bit of $c_{SFFI}$ is repeated by the factor of 30. Therefore, the encoded vector $X_{SFFI}$ is obtained (1*450). The BPSK constellation is mapped using equation $(-2 * X_{SFFI} + 1)(1+j)/\sqrt{2}$. It has a code rate $R_{SFFI}$ of 4/15. If the bits are repeated 30 times, $R_{SFFI}$ is given by 4/(15*30) = 1/450.

As per the annex [15], the length of SS ($L_{SS}$) of 495 symbols can be used for effective correlation which is calculated as 270 symbols from the SOSF and half of the 450 symbols from the SFFI i.e., 33 sub-blocks, each comprising 15 symbols.

## III. System Model

Consider the downlink received signal from the LEO communication satellite system with a specific frame format. The received signal at the front end, after filtering, down-conversion, and sampling, is expressed as:

$$r[n] = \sum_{k=1}^{N_{sat}} y_k[n] + \eta_k[n] \tag{8}$$

where, $r[n]$ is the sampled received signal, $\eta_k[n]$ represents additive noise, $N_{sat}$ is total number of visible satellites. The useful sampled signal, $y_k[n]$ is given by:

$$y_k[n] = A_k a_k(nT_s - \tau_k) e^{j(2\pi f_{d,k} n T_s + \phi)} \tag{9}$$

where, $A_k$ is signal amplitude from the $k$-th satellite, $\tau_k$ is the delay in the received signal from the $k$-th satellite, $f_{d,k}$ is the Doppler frequency affecting the $k$-th signal, $\phi$ is a random phase uniformly distributed in $[0, 2\pi]$, $T_s$ is the sampling interval.

$a_k$ represents the transmitted sequence from the $k$-th satellite, which includes the SS and data bits, which are defined as [16]:

$$a_k = \begin{cases} c_{l,k} & \text{if } l \in [0, L_{SS} - 1], \\ d_{l,k} & \text{if } l \in [L_{SS}, L_{SS} + L_{SF} - 1], \end{cases} \tag{10}$$

where $c_{l,k}$ is known SS, $d_{l,k}$ is unknown information bits, For DVB-S2X, the $L_{SS}$ is evaluated at 270, 495, 720, and 1023 symbols, to study its impact on acquisition performance and the data sequence $d_{l,k}$ derived from the remaining, $L_{SF} = 612540$ symbols. For GPS C/A (L1), $a_k = c_{l,k}$, representing the complete PRN code of 1023 chips.

### A. Statistical Signal Acquisition

In GNSS receivers, the acquisition phase identifies and synchronizes with signals from visible satellites, providing initial estimates of delay ($\hat{\tau}$) and Doppler ($\hat{f}_d$) [17]. These estimates are then refined during the tracking phase to generate accurate pseudorange or pseudorange rate measurements. In DVB-S2X, the acquisition plays a critical role in achieving initial synchronization, which can be done similarly to GNSS. This involves evaluating the Cross Ambiguity Function (CAF) in the time-frequency domain to obtain initial estimation of $\hat{\tau}$, $\hat{f}_d$. The CAF is computed as:

$$\begin{aligned} R(\tau, f_D) &= \frac{1}{L} \sum_{n=0}^{L-1} r[n]\, c[nT_s - \tau]\, e^{-j2\pi f_D n T_s} \\ \therefore [\hat{\tau}, \hat{f}_D] &= \arg \max_{(\tau, f_D)} |R(\tau, f_D)| \end{aligned} \tag{11}$$

where, $c$ is locally generated SS, $\tau$ and $f_D$ are chosen from finite 2D search space of [$L$, $N_f$] bins. In this way, the total number of hypotheses are $L \times N_f$ such that:

- The total number of delay bins, $L = T_{coh}/T_s$, where, $T_{coh}$ is coherent integration time.
- The total number of Doppler bins, $N_f = (f_{d,max} - f_{d,min})/\Delta f$, where $f_{d,max}$ and $f_{d,min}$ corresponds to maximum and minimum Doppler frequencies, respectively.
- Delay bins resolution, $\Delta\tau = f_{chip} \times T_s$, where $f_{chip}$ is chip or symbol frequency.
- Doppler bins resolution can be chosen using the thumb rule, $\Delta f_d \leq \frac{1}{2T_{coh}}$, which limits performance loss to under 3 dB that supports subsequent tracking stages [17]. In this way, $\tau = h\Delta\tau$, for $0 \leq h \leq L-1$; $f_D = l\Delta f_d$, for $0 \leq |l| \leq N_f/2$.

The CAF after averaging and enveloping coherently can be evaluated as follows:

$$S(\tau, f_D) = \left| \sum_{i=1}^{LNc} R^{(i)}(\tau, F_D) \right|^2 \tag{12}$$

Where $N_c$ is the total number of coherent integrations.

### B. Hypothesis Testing

Obtained search space $S(\tau, f_d)$ being evaluated over a finite and discrete delay and Doppler frequencies. Each cell can be represented by a random variable $s$, which is tested for two hypothesis tests [18]:

- $H_0$: Signal absent or misaligned.
- $H_1$: Signal present and synchronized.

Under $H_0$, Probability Density Function (PDF) of $S(\tau, f_d)|H_0$ is given by:

$$f_0(s) = \frac{1}{2\sigma_n^2} \exp\left(-\frac{s}{2\sigma_n^2}\right) \tag{13}$$

where $\sigma_n^2$ is the noise variance. The false alarm probability is given by [16]:

$$P_{FA}(\beta) = \int_{\beta}^{+\infty} f_0(s)\, ds = \exp\left\{\frac{-\beta}{2\sigma_n^2}\right\} \tag{14}$$

where $\beta$ is the decision threshold. So once the $P_{FA}$ is defined the $\beta$ can be estimated.

For $H_1$, PDF for $S(\tau, f_d)|H_1$ is equal to non-central chi-square distribution is given as:

$$f_1(s) = \frac{1}{2\sigma_n^2} \exp\left\{-\frac{s+\lambda}{2\sigma_n^2}\right\} I_0\left(\frac{\sqrt{s\lambda}}{\sigma_n^2}\right) \tag{15}$$

where $\lambda = A^2/2$ is the non-centrality parameter, $I_0$ is the modified Bessel function of the first kind and zero order [19]. Hence, the detection probability when the decision variable passes $\beta$ is given by:

$$P_D(\beta) = \int_{\beta}^{+\infty} f_1(s)\, ds = Q_1(a, b) \tag{16}$$

where $Q_1$ is Marcum function of the first order, [20] and $a$, $b$ are estimated by:

$$\begin{cases} a = \sqrt{\frac{\lambda}{\sigma_n^2}}, \\ b = \sqrt{\frac{\beta}{\sigma_n^2}} \end{cases} \tag{17}$$

In real scenarios, acquisition detection loses due to the delay and Doppler misalignment [21]. The effects of residual Doppler frequency ($\delta F$) and delay ($\delta\tau$) alignment error can be given by [18]:

$$\mathbb{L}(\delta\tau, \delta F) = \frac{\sin^2(\pi N \delta F)}{(\pi N \delta F)^2} R^2(\delta\tau). \tag{18}$$

Therefore, coherent output SNR becomes:

$$a = \sqrt{\frac{\lambda}{\sigma_n^2} \cdot \mathbb{L}(\delta\tau, \delta F)} \tag{19}$$

It is important to note that the frequency error, $\delta F$ is scaled by the factor $N$, representing the number of samples used for coherent integration of the input signal. Consequently, as the $T_{coh}$ increases, the impact of Doppler frequency residual errors becomes increasingly significant. To mitigate this effect, the Doppler bin size must be reduced as the $T_{coh}$ grows using the thumb rule [17].

### C. Mean Acquisition Time

MAT ($\bar{T}_A$) measures the average time required to acquire signal synchronization. This work considers the single-dwell acquisition structure, where $\bar{T}_A$ is computed as [15], [22]:

$$\bar{T}_A = (LN_f - 1)(T_d + T_{fa}P_{FA})\left(\frac{2 - P_D}{2P_D}\right) + \frac{T_d}{P_D} \tag{20}$$

where, $T_d$ is the dwell time, $T_{fa} = k_p T_d$ is the penalty time (with $k_p$ as the penalty coefficient). While this expression is specific to single-dwell scenarios, extensions to multi-dwell acquisition structures involve more complex probabilistic modeling and are planned for future studies. Overall, MAT reflects both the computational complexity and sensitivity of the acquisition strategy.

## IV. Performance Analysis

This section provides a detailed analysis of the ACF, ROC, and MAT for DVB-S2X and GPS C/A L1 waveforms. The analysis considers the acquisition losses as per Eq. 18.

| Parameters | GPS L1 C/A | DVB-S2X |
|---|---|---|
| **Frequency (MHz)** | L1 | S/C/Ku/Ka |
| **BW (MHz)** | 1.023 | 10 |
| **SNR (dB)** | -28.01 | -2.4 to 5.5 |
| **Length of Pilots** | 1023 Chips | SOSF: 270, SFFI: 420 symbols |
| **Pilot Duration / $T_{coh}$ (ms)** | 1 | 0.0252 |
| **Periodicity of Pilots (ms)** | 1 | 21.4 |
| **Multiple Access** | CDMA | TDMA, FDMA |
| **Modulations** | BPSK | BPSK, QPSK, 8PSK, 16, 32, 64, 128, 256 APSK |
| **Supported Platforms** | MEO | LEO, GEO, NGSO |

TABLE I: Signal properties of DVB-S2X and GPS L1 C/A useful for positioning.

Table I summarizes the key signal properties relevant to positioning estimation, such as signal BW, SS length and periodicity, operating SNR, multiple access schemes, modulation types, and supported platforms for both signals. For the GPS L1 C/A code, SS duration aligns with its periodicity, which is 1 ms and corresponds to $T_{coh}$. Instead, for DVB-S2X SS duration ($T_{coh}$) is 0.0252 ms and is determined by factors such as the roll-off factor, samples per symbol, BW, and the length of pilot sequences. It should be noted that SS exhibits strong autocorrelation and low cross-correlation properties for both signals, making them well-suited for initial synchronization. However, tight synchronization is less critical for communication applications [23] with respect to GNSS. Moreover, power is concentrated on the edges of the spectrum achieves better positioning performance, whereas in communication applications, power concentrated in the center of the spectrum is preferred to reduce inter-symbol interference [24].

In this paper, for DVB-S2X waveform, a LEO satellite at 1200 km altitude is considered with a frequency uncertainty of 20 ppm, and carrier frequency ($f_0$) is set to 2 GHz (S-Band), BW is set to 10 MHz as per the 3GPP specifications for LEO-NTN [25].

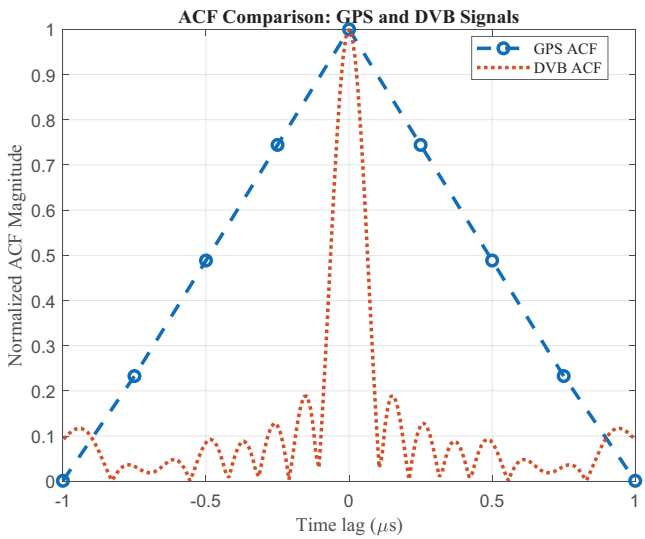


Fig. 2: Normalized ACF of GPS L1 (C/A code), DVB-S2X (SS) waveforms. Narrow main lobs for DVB-S2X due to higher BW

Fig. 2 presents the ACF of GPS C/A and DVB-S2X signals, reflecting their actual signal characteristics. The DVB-S2X ACF shows narrower main lobes compared to GPS C/A, which can be attributed to its higher signal BW. The length of SS does not affect the ACF, as both sequences show maximum ACF properties.

ROC analysis is essential for evaluating acquisition performance in noisy environments. Since the operating SNR (C/N0) varies between GPS C/A L1 and DVB-S2X signals, ROC curves are derived for both systems using Eq. 14 and Eq. 16. Monte Carlo simulations are conducted to ensure statistical reliability. The ROC curves are generated based on signal BW, C/N0, SS lengths, $T_{coh}$, etc. Fig. 3 and 4 demonstrate the

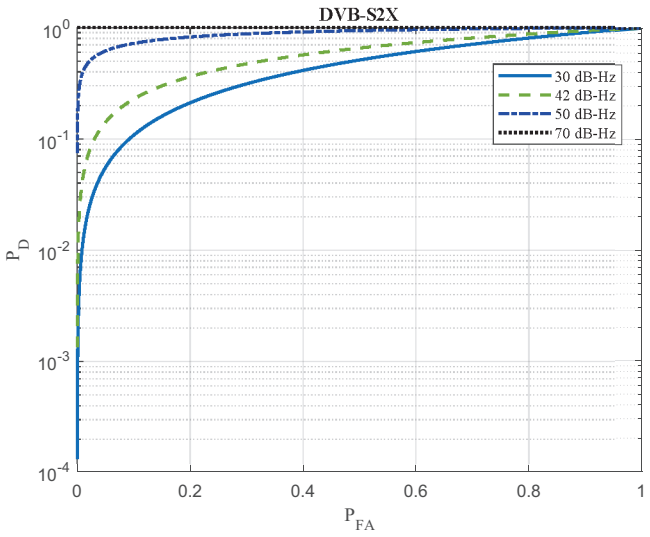


Fig. 3: ROC of DVB-S2X for BW of 10 MHz with acquisition losses.

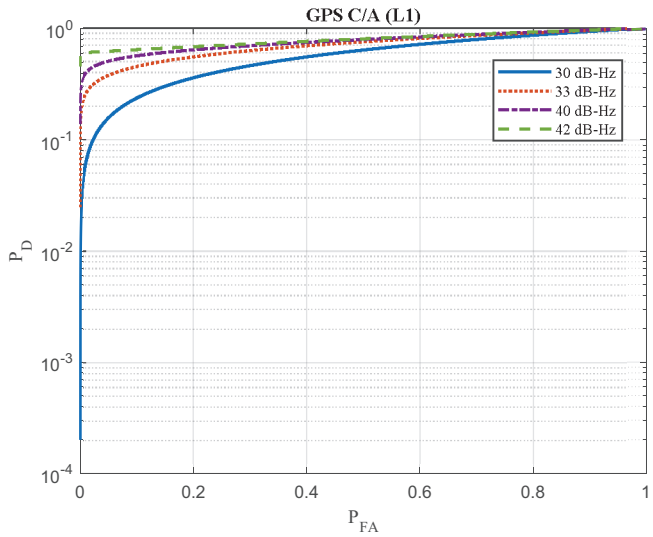


Fig. 4: ROC of GPS C/A code for BW of 1.023 MHz with acquisition losses.

ROC curves of both DVB-S2X and GPS C/A L1 code, which are plotted for actual signal properties, i.e., operating $C/N_0$ and BW. Due to the distinct characteristics of the two signals, the corresponding curves are plotted on separate figures rather than within a single plot. As DVB-S2X operates at higher $C/N_0$ (above 50 dB-Hz) than GPS C/A L1, resulting in better signal detection. At $C/N_0$ of 30 and 42 dB-Hz, GPS C/A L1 shows slightly better detection at $P_{FA}$ of 0.2 compared to DVB-S2X. This is due to the longer PRN length than the SS of DVB-2X, which is 495 in this case. It should be noted that the obtained ROCs consider the aforementioned acquisition losses. In the case of GPS C/A L1, ROC without losses is matched to the results obtained by the author [18]. In this way, DVB-S2X shows better acquisition performance due to higher signal BW and operating $C/N_0$.

Fig. 5 further examines the effect of SS length on ROC performance at constant C/N0 of 42 dB-Hz and $T_{coh}$ set equal to the duration of SS. It can be seen that better detection can be achieved with longer SS. At $P_{FA}$ of 0.4, SS of 720 and 1023 symbols show similar performance as that of PRN of 1023 chips. This highlights the trade-off between SS length and detection performance under specific signal conditions.

Finally to estimate the MAT, $T_d$ is set to the frame period $T_{SF}$, as the synchronization pattern is not transmitted continuously as in GNSS. The term $(T_{fa}.P_{FA})$ is close to zero. It is assumed that leveraging a Fast Fourier Transform (FFT) - based search enables simultaneous exploration of all time hypotheses, leaving only the frequency hypotheses to be searched sequentially.

Fig. 6 shows MAT variation for different SS lengths for constant $P_{FA}$ = 0.01. $T_{coh}$ is set to the duration of the given SS. It can be seen that at a low $C/N_0$ of 30 dB-Hz, MAT is about 100 sec, after 50 dB-Hz it drops well below 10 sec for any SS length, which is the operating range of the DVB-S2X

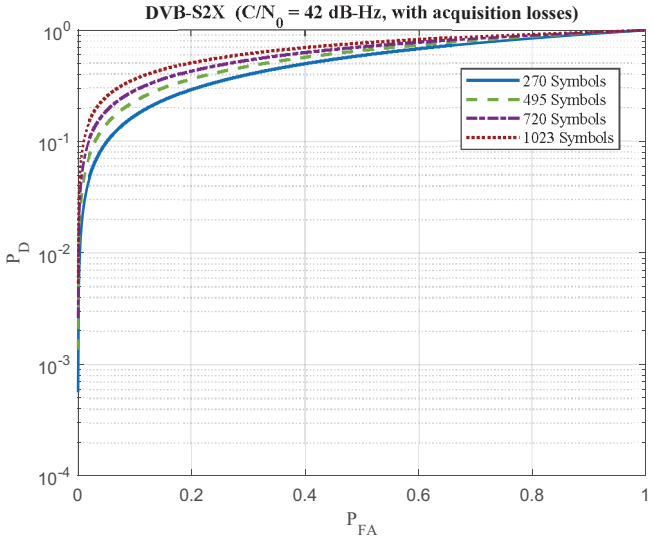


Fig. 5: Effect of length of SS on DVB-S2X ROC for C/No of 42 db-Hz

signal. Specifically, at 50 dB-Hz MAT for SS of 270 symbols is the highest due to lower $P_D$ and least for 1023 symbols due to better $P_D$.

In this way, the influence of $C/N_0$, SS length, and acquisition losses due to longer $T_{coh}$ on MAT performance, highlights the trade-off between signal robustness and acquisition time under varying conditions. Optimal coherent integration length can be selected based on the coherent integration length dimensioning rule [26].

## V. Conclusion

This study provides a preliminary analysis of the potential for using the DVB-S2X protocol in LEO-PNT applications

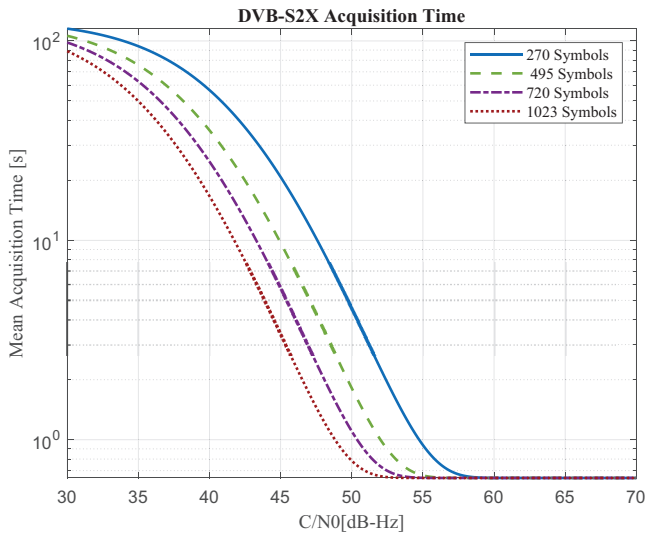


Fig. 6: Mean Acquisition Time (MAT) for constant $P_{FA}$ = 0.01

within NTN. GNSS, like statistical acquisition analysis, validates the feasibility of re-purposing DVB-S2X superframes for positioning tasks. High-operating SNR and BW can be beneficial for integrated Nav-Comm applications. However, a trade-off shall be made based on the synchronization sequence length, coherent integration time, and acquisition losses to utilize for dual purposes. Future work will concentrate on optimizing these parameters for positioning and their effects on communication services in multi-satellite scenarios under various operational conditions, impact of shorter duration of a LEO satellite than a MEO satellite on coherent integration, along with comparing them with positioning performance obtained by the SoO of 5G-NR (use of SSB for acquisition and tracking), dedicated PRS (use of SSB for acquisition and PRS for tracking), and other GNSS waveforms.

## REFERENCES


[1] E. C. H. More and M. D. Sanctis, "Comparing positioning performance of leo mega-constellations and gnss in urban canyons," *IEEE Access*, vol. 12, pp. 24 465–24 482, 2024.

[2] P. A. Iannucci and T. E. Humphreys, "Fused low-earth-orbit gnss," *arXiv: Signal Processing*, Nov 2020, 2020b.

[3] P. Iannucci and T. Humphreys, "Economical fused leo earth orbit gnss," in *IEEE/ION Position, Location and Navigation Symposium (PLANS)*, Apr 2020.

[4] H. More, F. Menzione, O. M. Picchi, M. De Sanctis, and E. Cianca, "Leveraging 5g-nr and dvb-s2x for positioning in leo-ntn," in *Proceedings of the 2025 International Technical Meeting of The Institute of Navigation*, Long Beach, California, Jan. 2025, pp. 139–150.

[5] ESA, "Multi-access relative performance comparison for gso broadband satellite networks (marina)," 2023. [Online]. Available: https://connectivity.esa.int/projects/marina

[6] T. Huikko, "Comparison of 5g nr and dvb-s2x/rcs2 technologies in broadband satellite systems," Technical Report or similar description, 2023.

[7] S. Chen, S. Sun, and S. Kang, "System integration of terrestrial mobile communication and satellite communication -the trends, challenges and key technologies in b5g and 6g," *China Communications*, vol. 17, no. 12, pp. 156–171, 2020.

[8] ETSI-EN-302-307, "Digital video broadcasting (dvb); second generation framing structure, channel coding and modulation systems for broadcasting, interactive services, news gathering and other broadband satellite applications (dvb-s2)," ETSI, Tech. Rep., 2013.

[9] ETSI-EN-302-307-2, "Digital video broadcasting (dvb); second generation framing structure, channel coding and modulation systems for broadcasting, interactive services, news gathering, and other broadband satellite applications; part 2: Dvb-s2 extensions (dvb-s2x)," ETSI, Tech. Rep., 2015, version 1.1.1.

[10] K. Shamaei and Z. Kassas, "Receiver design and time of arrival estimation for opportunistic localization with 5g signals," *IEEE Transactions on Wireless Communications*, vol. PP, pp. 1–1, 2021.

[11] 3GPP-PRS, "Physical channels and modulation (release 16)," 3GPP, Tech. Rep., Dec 2019, version 16.0.0.

[12] "Digital video broadcasting (dvb); second generation framing structure, channel coding and modulation systems for broadcasting, interactive services, news gathering, and other broadband satellite applications; part ii: S2-extensions (s2-x)," 2014, standard.

[13] A. Hedayat and W. D. Wallis, "Hadamard matrices and their applications," *The Annals of Statistics*, pp. 1184–1238, 1978.

[14] H. Zhang and F. Ding, "On the kronecker products and their applications," *Journal of Applied Mathematics*, vol. 2013, 2013.

[15] ETSI-TR-102, "Digital video broadcasting (dvb); implementation guidelines for the second-generation system for broadcasting, interactive services, news gathering and other broadband satellite applications; part 2: S2 extensions (dvb-s2x)," ETSI, Tech. Rep., 2021, version 1.2.1.

[16] N. Mazzali, G. Stante, S. M. R. R. Bhavani, and B. Ottersten, "Performance analysis of noncoherent frame synchronization in satellite communications with frequency uncertainty," in *2015 IEEE Symposium on Communications and Vehicular Technology in the Benelux (SCVT)*, 2015, pp. 1–6.

[17] E. D. Kaplan, J. Christopher, and Hegarty, *Understanding GPS: Principles and applications. (second revised edition)*. New York: Artech House, 2017.

[18] D. Borio, "A statistical theory for gnss signal acquisition," Ph.D. dissertation, Politecnico di Torino, 2008.

[19] M. Abramowitz and I. A. Stegun, *Handbook of Mathematical Functions with Formulas, Graphs, and Mathematical Table*, M. Abramowitz and I. A. Stegun, Eds. Dover Publications, Jun. 1965.

[20] J. Marcum, "Table q-functions," U.S. Air Force Project RAND, Tech. Rep., 1950, aSTIA document AD 1165451.

[21] B. Parkinson and J. J. Spilker, *Global Positioning System: Theory and Applications*. American Institute of Aeronautics and Ast (AIAA), 1996, vol. 1st.

[22] S. H. Park, I. H. Choi, S. J. Lee, and Y. B. Kim, "A novel gps initial synchronization scheme using decomposed differential matched filter," in *Proceedings of ION NTM 2002*, San Diego, CA, USA, 2002, pp. 246–253.

[23] K. Shamaei and Z. M. Kassas, "Receiver design and time of arrival estimation for opportunistic localization with 5g signals," *IEEE Transactions on Wireless Communications*, vol. 20, no. 7, pp. 4716–4731, Jul 2021.

[24] S. E. Trevlakis, A.-A. A. Boulogeorgos, D. Pliatsios, J. Querol, K. Ntontin, P. Sarigiannidis, S. Chatzinotas, and M. Di Renzo, "Localization as a key enabler of 6g wireless systems: A comprehensive survey and an outlook," *IEEE Open Journal of the Communications Society*, vol. 4, pp. 2733–2801, 2023.

[25] 3GPP, "Technical specification group radio access network; nr; physical channels and modulation (release 17)," 3GPP, Tech. Rep., 2022, version 17.7.0.

[26] G. Corazza, R. Pedone, and M. Villanti, "Frame acquisition for continuous and discontinuous transmission in the forward link of satellite systems," *International Journal of Satellite Communications and Networking*, vol. 24, pp. 185 – 201, 03 2006.